Giant magnetic hardening of a Fe-Zr-B-Cu amorphous alloy during the first stages of nanocrystallization

C. Gómez-Polo
Departamento de Física de Materiales and Instituto de Magnetismo Aplicado (UCM), Instituto de Ciencias de Materiales, Consejo Superior de Investigaciones Científicas, P.O. Box 155, 28230 Las Rozas, Madrid, Spain

D. Holzer
Institute für Experimentalphysik, Technische Universität Wien, 1040 Wien, Austria

M. Multigner
Departamento de Física de Materiales and Instituto de Magnetismo Aplicado (UCM), Instituto de Ciencias de Materiales, Consejo Superior de Investigaciones Científicas, P.O. Box 155, 28230 Las Rozas, Madrid, Spain

E. Navarro
Sección departamental de Física Aplicada, Facultad de Veterinaria, UCM, Instituto de Ciencias de Materiales, Consejo Superior de Investigaciones Científicas, P.O. Box 155, 28230 Las Rozas, Madrid, Spain

P. Agudo, A. Hernando, and M. Vázquez
Departamento de Física de Materiales and Instituto de Magnetismo Aplicado (UCM), Instituto de Ciencias de Materiales, Consejo Superior de Investigaciones Científicas, P.O. Box 155, 28230 Las Rozas, Madrid, Spain

H. Sassik and R. Grössinger
Institute für Experimentalphysik, Technische Universität Wien, 1040 Wien, Austria
(Received 16 May 1995)

The coercive field of $Fe_{87.2}Zr_{7.4}B_{4.3}Cu_{1.1}$ amorphous ribbons obtained by melt spinning becomes 1 A m^{-1}, in the relaxed state, which is achieved after annealing at 410 °C during 1 h. After annealing for the same time at 480 °C the coercive force abruptly increases up to 100 A m^{-1}. For increasing annealing temperatures the coercivity drops again to 10 A m^{-1}. X-ray diffraction and Mössbauer spectroscopy show that the magnetic hardening is due to the appearance of a few nanocrystals of Fe which are separated a distance that in average is longer than the exchange correlation length of the amorphous matrix. As the number of Fe nanocrystals increase, the intergranular distances decrease and the grains become exchange coupled giving rise to the subsequent magnetic softening.

I. INTRODUCTION

A new group of nanocrystalline ferromagnets obtained by crystallization of the amorphous state constitute an interesting object for fundamental studies of magnetism in heterogeneous structures. In particular those Fe-rich nanocrystalline materials, as Fe-Si-B-Cu-Nb, have been shown to exhibit excellent soft magnetic properties.[1]

Herzer[2] has successfully applied the Alben-Becker-Chi model[3] to explain the grain-size dependence of coercivity. Even though the random anisotropy model developed in Ref. 3 considered single magnetic phase systems, the behavior of the two-phase nanocrystalline samples is well described by the model. For nanocrystalline materials the exchange between the anisotropic grains should take place through the amorphous matrix. However, as the exchange correlation length of the amorphous matrix is, in general, longer than the intergranular average distance, the grains are coupled and behave similarly to single-phase systems. There are two situations for which the two phase character of nanocrystalline samples turns out to be relevant. The first corresponds to the initial stage of nanocrystallization, when the average distance between grains is larger than the exchange-correlation length of the amorphous structure. For this case the domain-wall thickness is smaller than the distance between grains and they act as pinning centers. The second case is related to the thermal dependence of the magnetization process. As the Curie temperature of the amorphous phase is lower than that of the nanocrystals, the coupling between different grains disappears when the temperature reaches the Curie temperature of the amorphous intergranular region.

II. EXPERIMENTAL TECHNIQUES

Ribbons, with typical thickness of 23 μm and nominal composition $Fe_{87.2}Zr_{7.4}B_{4.3}Cu_{1.1}$, were rapidly solidified by the melt-spinning technique. Conventional isochronal thermal treatments (1 h) were performed in Ar atmosphere in a range of annealing temperatures from 400 to 650 °C. The crystallization process was followed by x-ray diffraction (SIEMENS D-5000) and differential scanning calorimetry (DSC), using a Perkin-Elmer DSC-7 calorimeter.

Mössbauer experiments were performed at room temperature using a Co source in a Rh matrix. The isomer shift

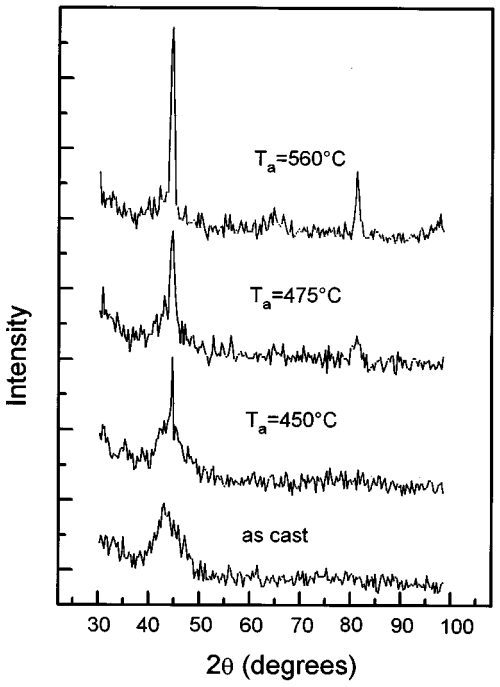

FIG. 1. Evolution of x-ray-diffraction patterns with annealing temperature T_a.

values are given relative to the center of the α-Fe spectrum. With respect to the magnetic properties, axial hysteresis loops were obtained at different measuring temperatures (up to 550 °C) using a conventional induction method that allowed the determination of the temperature dependence of typical magnetic parameters such as coercive field H_c and saturation magnetization M_s. The analysis of the thermal behavior of M_s at low temperatures (from 5 to 300 K) was performed by superconducting quantum interference device magnetometry (Quantum Desing MPMS) under a magnetic field of 5 T.

III. RESULTS

The evolution of the x-ray-diffraction patterns with the annealing temperature, T_a, is plotted in Fig. 1, the sample in as-cast state presents a typical amorphous halo. The occurrence of crystallization peaks, corresponding to α-Fe phase, is detected for annealing temperatures above 450 °C. From the Sherrer formula, the mean grain diameter $\langle\delta\rangle$ of the crystalline phase can be estimated (see Table I). Surprisingly, $\langle\delta\rangle$ presents a maximum value equal to 22.8 nm at the beginning of the crystallization process ($T_a=450$ °C), followed by a continuous decrease with the annealing temperature.

TABLE I. Mean grain diameter $\langle\delta\rangle$ versus annealing temperature T_a.

T_a (C)	$\langle\delta\rangle$ (nm)
450	22.8
475	13.5
560	12.9
603	12.7

TABLE II. Peak enthalpy (J/g) corresponding to the α-Fe crystallization peak as a function of the annealing temperature T_a.

T_a (C)	Peak enthalpy (J/g)
as-cast	68
450	68
475	55
500	1
560	0

This behavior can be interpreted as a consequence of the appearance of a superficial crystalline fraction at the first stages of the crystallization. Moreover, the occurrence of a single (110) reflection for $T_a=450$ °C clearly indicates a preferential crystalline growth. From $T_a=560$ °C, $\langle\delta\rangle$ presents a constant value close to 13 nm that would correspond with the mean grain size of the homogeneous crystallization in the bulk of the sample.

DSC scans support the above conclusions. Firstly, the crystallization process takes place in two main steps.[4,5] The precipitation of the α-Fe phase occurs for T_a close to 560 °C. For higher annealing temperatures ($T_a>700$ °C), new crystalline phases, mainly Fe-Zr phases, complete the crystallization process. If the DSC thermographs are analyzed for the as-cast and previously thermally treated samples, the volume fraction associated with the first crystallization process can be estimated from the corresponding peak area. As Table II shows, the crystallization process starts for annealing temperatures higher than 450 °C. In fact, for T_a above 560 °C the first crystallization process associated with the precipitation of the α-Fe phase has completely finished.

With respect to the influence of the detected changes in structure on the magnetic properties of the samples, Fig. 2 shows the dependence of the coercive field H_c with T_a measured at room temperature. As can be seen, the soft magnetic behavior of the as-cast sample is dramatically deteriorated for T_a around 475 °C. This magnetic hardening should be associated with the first stages of crystallization process. Nevertheless, for further annealings above 525 °C, where the homogeneous α-Fe nanocrystalline phase is precipitated,

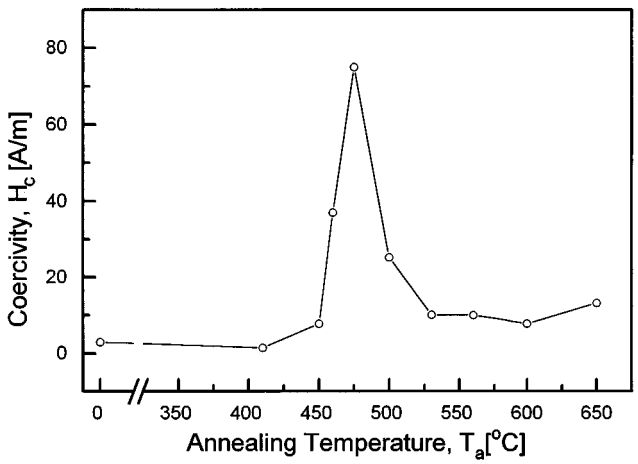

FIG. 2. Room-temperature coercive field H_c versus annealing temperatures T_a.

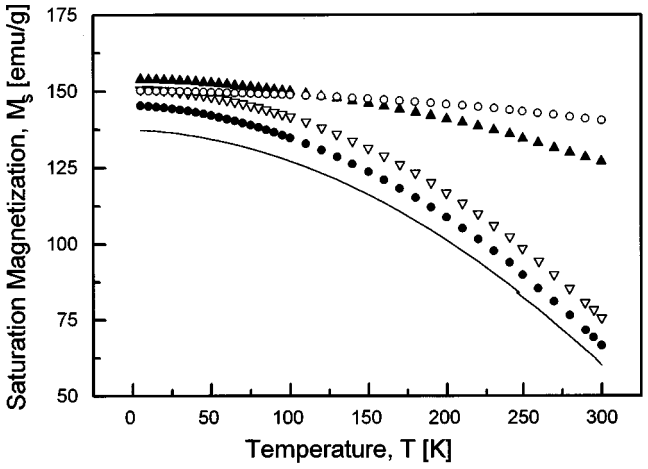

FIG. 3. Thermal dependence of saturation magnetization, M_s, at low measuring temperature T: (●) as-cast, (—) $T_a=410$ °C, (▽) $T_a=475$ °C, (▲) $T_a=500$ °C, and (○) $T_a=603$ °C.

H_c presents similar low values to the as-cast state. This magnetic softening must be interpreted within the framework of the random anisotropy model as has been previously pointed out.[2]

The superficial and preferential crystalline growth at the first stages of nanocrystallization could be invoked as the main origin of the detected increase in H_c for $T_a>400$ °C. To estimate its contribution to the observed magnetic hardening, the sample annealed at 450 °C was chemically etched in order to remove the superficial crystalline layer of the sample. Under these circumstances, the previously detected texture is negligible after the etching. Moreover, $\langle\delta\rangle$ decreases reaching a mean value of 5 nm. The most remarkable result is the fact that the coercivity does not significantly change. Therefore, we can conclude that the origin of the detected magnetic hardening should not be related to this preferential crystalline effect.

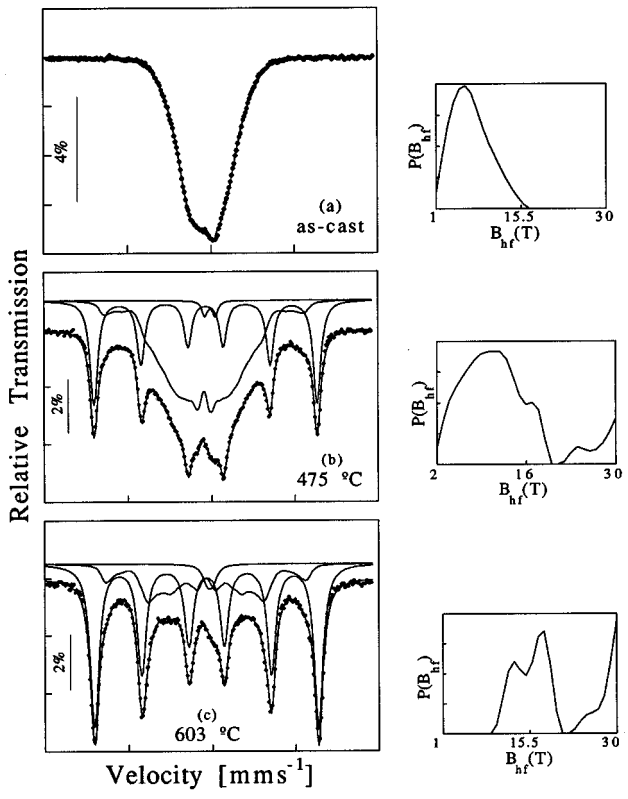

FIG. 4. Mössbauer spectra of the as-cast (a) and thermally treated samples [(b) $T_a=475$ °C and (c) $T_a=603$ °C].

TABLE III. Bloch law fitting parameters, $M_s=M_s(0)\times(1-BT^{3/2}-CT^{5/2})$, versus annealing temperature T_a.

T_a (C)	M_s (emu/g)	B (K)$^{-3/2}$	C (K)$^{-5/2}$
as-cast	115.6	5.97×10^{-5}	1.50×10^{-7}
410	137.8	6.30×10^{-5}	1.53×10^{-7}
450	146.8	5.74×10^{-5}	1.60×10^{-7}
475	151.11	4.71×10^{-5}	1.65×10^{-7}
500	154.0	2.27×10^{-5}	0.38×10^{-7}
603	150.2	0.66×10^{-5}	0.19×10^{-7}

However, a change in the magnetic nature of the residual amorphous matrix can be thought to be responsible of the described phenomenon. The analysis of the thermal dependence of the saturation magnetization, M_s, for the as-cast and annealed samples reveals no significant changes in the magnetic moment at low temperatures (see Fig. 3). The experimental data can be fitted to the Bloch law, written as follows:

$$M_s(T)=M_s(0)(1-BT^{3/2}-CT^{5/2}), \tag{1}$$

where $M_s(0)$ is the saturation magnetization at 0 K, and B and C are characteristic constants of spin-wave excitations.[6] Table III displays the fitting parameters for the as-cast and annealed samples. As the crystalline volume fraction increases with the annealing temperature ($T_a>475$ °C), B decreases approaching the limiting value of α-Fe pure phase ($B_{\mathrm{Fe}}=7.5\times10^{-6}$ K$^{-3/2}$).

From Mössbauer spectrometry deeper information about the structural changes that take place during the crystallization process can be obtained.[7,8] Figure 4 shows the Mössbauer spectra for the as-cast and thermally treated samples. The as-cast and structurally relaxed amorphous samples ($T_a<460$ °C) present a broad line, characteristic of a hyperfine field distribution of a disordered ferromagnetic structure. Table IV summarizes the fitting parameters as a function of the annealing temperature. As the amorphous structure relaxes (up to $T_a=460$ °C) the mean hyperfine field, $\langle B_{\mathrm{hf}}\rangle$, slightly increases. Nevertheless, it is important to remark that in this T_a range, $\langle B_{\mathrm{hf}}\rangle$ does not reach very high values. Once the crystallization process starts ($T_a>475$ °C), the experimental data can be fitted to three different subspectra: the residual amorphous matrix, the sextet characteristic of the precipitated α-Fe crystalline phase and a doublet that must be associated with a nonferromagnetic Fe phase. The obtained hyperfine field, B_{hf}, of the sextet, close to 33 T, together with the nearly zero values of the quadrupole and isomer shift, reveal that the crystalline ferromagnetic grains are mainly composed by an α-Fe pure phase.

TABLE IV. Evolution of hyperfine parameters and relative areas obtained from the Mössbauer spectra, as a function of the annealing temperature T_a (IS: isomer shift; B_{hf}: hyperfine magnetic field; QS: quadrupole; Ra: resonant area).

T_a (C)	Phases	IS (mm s^{-1})	B_{hf} (T) [a]	QS (mm s^{-1})	Ra (%)
As-cast	Amorp-ferro	−0.031	6.9	0.14	100
410	Amorp-ferro	−0.048	5.6	−0.12	100
450	Amorp-ferro	−0.019	6.3	−0.14	100
460	Amorp-ferro	0.022	6.8	0.14	100
475	Amorp-ferro	−0.073	12.3	0.06	64
	α-Fe	0	32.9	0.003	34
	Nonferrom.	0.2		−0.49	2
500	Amorph-ferro	−0.05	11.5	0.17	64
	α-Fe	0	32.89	0.008	32
	Nonferrom.	0.003		−0.46	3
530	Amorph-ferro	−0.053	13.5	0.15	41
	α-Fe	0.004	32.9	0.10	56
	Nonferrom.	−0.008		−0.37	3
560	Amorph-ferro	0.104	17.2	0.17	39
	α-Fe	0.01	32.8	−0.006	56
	Nonferrom.	−0.014		−0.32	5
603	Amorp-ferro	−0.024	19.5	−0.10	29
	α-Fe	0.005	33	0.003	68
	Nonferrom.	0.158		0.24	3

[a] B_{hf} is the hyperfine magnetic field of the crystalline phase of α-Fe or the average hyperfine magnetic-field distribution $\langle B_{hf} \rangle$ of the amorphous ferromagnetic phase.

IV. DISCUSSION

It is important to remark that the maximum value of H_c corresponds with a low ferromagnetic crystalline volume fraction ($\sim$35%). This last result clarifies the origin of the detected magnetic hardening. According to the random-anisotropy model, the anisotropy of this multiphase system averages out when the exchange correlation length, L_0, dominates the orientation fluctuation length δ of randomly distributed local easy axis ($L_0 > \delta$). Accordingly,[2] L_0 can be expressed as follows:

$$L_0 = 16A^2/9K^2\delta^3, \tag{2}$$

where A and K are the exchange and magnetocrystalline anisotropy constants of crystallites, respectively.

In a multiphasic system composed by crystalline grains immersed in an amorphous matrix, this theory is only valid when the crystalline fraction x is equal to 1 (fully crystallized sample) or when the exchange-correlation length of the amorphous matrix L_{am} tends to infinity. However, in those intermediate cases, that is, low values of x or finite values of L_{am}, the theory must be modified. As has been pointed out by Hernando *et al.*[9] the exchange constant A must be substituted by γA where γ is a parameter varying between 0 and 1, expressed as

$$\gamma = e^{-\Lambda/L_{am}}, \tag{3}$$

where Λ, the average distance between the surface of two adjacents crystallites, can be easily estimated as

$$\Lambda = \delta(1/x)^{1/3} - \delta. \tag{4}$$

According to this theory, the condition required for the macroscopic structural anisotropy to decrease respect to K is

$$(4A/3K) > (\delta^2 x^{3/2}/\gamma), \tag{5}$$

and the maximum size of crystallites verifying the above condition δ^* would depends on x as

$$\delta^* = \delta_0 \gamma / x^{1/3}, \tag{6}$$

where δ_0 is the maximum size verifying $L_0 > \delta$ for $x = 1$.

For mean grain sizes higher than δ^*, the grains are decoupled and their magnetization follows the easy-axis direction determined by the magnetocrystalline anisotropy, giving rise to a magnetic hardening of the sample. An exact calculation of δ^* implies the determination of L_{am} through γ parameter [see Eqs. (3) and (6)]. A rough estimation of L_{am} can be done through the following expression:

$$L_{am} = (A_{am}/K_{am})^{1/2}, \tag{7}$$

where A_{am} and K_{am} correspond to the exchange and anisotropy constants of the amorphous phase. The value of K_{am} can be evaluated through the magnetization work. In this particular case, the as-cast sample presents a value of K_{am} of 100 J/m^3. Under these assumptions and after estimating A_{am} through the Curie temperature of the amorphous phase ($T_C \approx 310$ K), we obtain that L_{am} (≈ 0.5 μm) gives always rise to δ^* values higher than the mean crystalline size ($\delta \approx 13$ nm) for all the crystalline fraction values. Therefore, a complete exchange coupling between the grains is expected to occur within the whole range of annealing temperatures, and the maximum of coercivity cannot be explained.

However, the crystallization process can introduce in the amorphous phase strong internal stresses that could drastically increase the effective K_{am} value, and so significantly decrease of L_{am}. A reduction of L_{am} up to 5 nm would imply values of internal stresses around 1000 MPa. This estimated L_{am} would lead to δ^* values contained between 12 and 14 nm for annealing temperatures of 475 and 560 °C, respectively. Therefore, for $T_a = 475$ °C the magnetic grains would be decoupled as a consequence of the condition $\delta > \delta^*$, though for higher annealing temperature, the magnetic softening must be interpreted as the result of $\delta < \delta^*$. Nevertheless, for higher T_a (≈ 603 °C) and assuming L_{am} constant and equal to 5 nm, δ^* decreases and the condition $\delta < \delta^*$ is no longer valid. It is important to point out that the assumption that L_{am} remains constant with thermal treatments is not completely correct. In fact, the increase of the mean hyperfine field, $\langle B_{\mathrm{hf}} \rangle$, of the amorphous phase obtained from the Mössbauer spectra indicates that the crsytallization process effectively influences L_{am} (see Table IV). Disregarding the exact correlation between $\langle B_{\mathrm{hf}} \rangle$ and L_{am}, what can be concluded is that the crystallization process must cause a noticeable increase in L_{am}. Just assuming that L_{am} increases as much as twice (≈ 10 nm) and by considering the actual values of Λ and x for $T_a = 603$ °C, δ^* reaches a value of 20 nm, so the condition for coupling between grains is fully verified.

The occurrence of a nonmagnetic Fe phase in the partially crystallized samples, as is concluded from the Mössbauer analysis, could also contribute to the decoupling between the ferromagnetic grains and thereby to the observed magnetic hardening. Nevertheless, its low mean volume fraction ($\sim 3\%$), besides the fact that their maximum values are obtained for those T_a where the softest magnetic behavior is found ($T_a \sim 560$ °C), indicates that the effect of this nonferromagnetic phase does not significantly contribute to the hardening effect. However, it can play an improtant role in the decrease of the estimated L_{am}. In fact, it is very reasonable to assume that this nonferromagnetic phase is distributed at the interphase between the ferromagnetic Fe grains and the residual amorphous matrix. Its existence would partially shield the exchange penetration through the amorphous matrix and would give rise to a decrease in the effective value of L_{am}.

The evolution of the coercivity with the annealing temperature can be summarized as follows: at the beginning of the crystallization process ($T_a \approx 450$ °C) the ferromagnetic grains are magnetically decoupled and the magnetization within the grains follows the easy axis determined by the magnetocrystalline anisotropy. At this stage, the domain-wall movements dominate the magnetization process within the residual amorphous matrix. Under these circumstances, the small crystalline granules act as pinning centers for the domain walls that mainly determine the value of coercivity in this two multiphase system, so giving rise to the observed magnetic hardening. As the crystallization process proceeds and the crystalline fraction increases, the intergranular distances decrease and the magnetic coupling between the grains becomes effective, causing a macroscopic magnetic softening.

Finally, in order to deepen into the intergranular interaction and its correlation with the annealing temperatures, the dependence of M_s and H_c was evaluated as function of the measuring temperature T (from 300 to 550 °C). The results are summarized in Figs. 5(a) and 5(b). The main characteristic of the thermal dependence of H_c is the occurrence of a maximum for a certain value of T. For those annealed samples with higher crystalline fraction and low values of coercivity ($T_a = 500$ and 530 °C), the appearance of this maximum should be associated with the decoupling of the ferromagnetic grains as a consequence of the matrix transition to its paramagnetic state.[10] Under these circumstances, the parameter γ tends to zero, giving rise to nearly zero values of L_{am} and to a drastic increase in the critical δ^* size. However a sharp maximum is also observed for lower annealing temperatures, for which the grains are uncoupled at room temperature, as discussed above. Therefore the decoupling between grains cannot be invoked as cause of the appearance of the maximum. In this case and as has been previously described, the magnetization process at room temperature is mainly determined by the domain-wall movement of the residual amorphous matrix and the contribution of the decoupled ferromagnetic grains can be considered negligible. However, as the matrix tends to its paramagnetic state, the contribution of the ferromagnetic grains to the magnetization process and consequently to coercivity becomes more noticeable, giving rise to very high values of H_c (~ 1800 A/m). For further measuring temperatures above the Curie point of the residual amorphous matrix H_c sharply

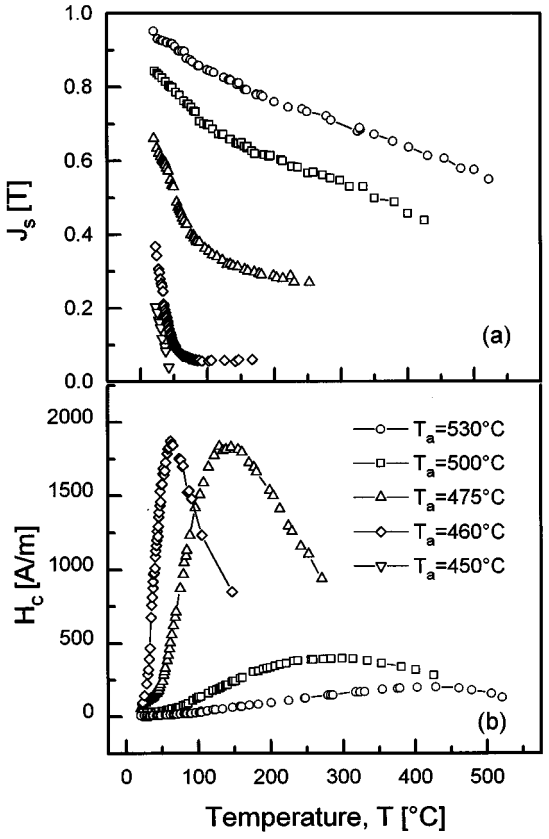

FIG. 5. Evolution of (a) saturation magnetization, M_s, and (b) coercive field H_c, versus measuring temperature T: ($\triangledown$) $T_a = 450$ °C, ($\diamond$) $T_a = 460$ °C, ($\triangle$) $T_a = 457$ °C, ($\square$) $T_a = 500$ °C, and ($\bigcirc$) $T_a = 530$ °C.

decreases. This behavior could be associated with the superparamagnetic nature of the precipitated Fe granules.[11]

V. CONCLUSIONS

It is well known that FeZrB alloys presents a magnetic softening after partial crystallization. Such a behavior has been correlated to the precipitation of an homogeneous α-Fe nanostructure. The random anisotropy model has been used as an approximation to explain the exchange interaction between α-Fe grains as the main origin of the observed magnetic softening. However this approximation is valid only in two limiting cases: for fully crystallized samples or L_{am} tends to infinity. But for intermediate cases, that is, first stages of crystallization and near the Curie point of the matrix ($L_{\mathrm{am}} \approx 0$), this model must be modified.

In this work, these intermediate situations are studied. The evolution of coercivity with annealing temperature, is analyzed in order to clarify the changes that take place in the exchange interactions between grains, with the crystalline fraction and intergranular distances compared to the matrix exchange correlation length. The results show that a giant magnetic hardening is observed for low crystalline fraction (low annealing temperature) as a consequence of too high grain interdistances. As the crystalline fraction increases, but the mean grain size remains almost constant, the exchange coupling becomes more effective and a significant magnetic softening is observed. Such a behavior is explained taking into account the modifications that must be introduced on the random-anisotropy model due to the two-phase nature of the system. Moreover, the nonmagnetic detected intergranular phase plays an important role in the exchange interaction between the α-Fe grains and the residual amorphous matrix, partially shielding such an interaction.

The other limiting cases (L_{am} tends to zero) is also analyzed through the study of the thermal dependence of coercivity close to the Curie point of the matrix. Its transition to a paramagnetic state gives rise to a decoupling of the ferromagnetic grains, and so a maximum in the coercivity values. The subsequent decrease with the measuring temperature is a direct consequence of the superparamagnetic nature of the grains, though strong magnetostatic interaction are detected for higher crystalline fractions.

ACKNOWLEDGMENTS

This work has been performed within the framework of *Agreement for Research Cooperation* between the Austrian and Spanish Ministries of Foreign Affairs, and supported by IBERDROLA S.A. and the Spanish C.I.C.Y.T. under Projects No. MAT 92-0156, No. MAT92-0405, and No. MAT 92-491.

[1] Y. Yoshizawa, S. Oguma, and K. Yamauchi, J. Appl. Phys. **64**, 6044 (1988).

[2] G. Herzer, IEEE Trans. Magn. **25**, 3327 (1989); Mater. Sci. Eng. A **133**, 1 (1991); Phys. Scr. T **49**, 307 (1993).

[3] R. Alben, J. J. Becker, and M. C. Chi, J. Appl. Phys. **49**, 1653 (1978).

[4] K. Suzuki, N. Katoaka, A. Inoue, A. Makino, and T. Masumoto, Mater. Trans. JIM **31**, 743 (1990).

[5] K-S. Kim and S-C. Yu, IEEE Trans. Magn. **29**, 2679 (1993).

[6] A. Herpin, *Theorie du magnetisme* (Presses Universitaires de France, Paris, 1968), pp. 389–420.

[7] I. Navarro, A. Hernando, M. Vázquez, and S-C. Yu, J. Magn. Magn. Mater. **145**, 313 (1995).

[8] P. Gorria, I. Orue, F. Plazaola, and J. M. Barandiarán, J. Appl. Phys. **73**, 6600 (1993).

[9] A. Hernando, M. Vázquez, T. Kulik, and C. Prados, Phys. Rev. B **51**, 3581 (1995).

[10] A. Slawska-Wanieska, P. Nowicki, H. K. Lachowicz, P. Gorria, J. M. Barandiarán, and A. Hernando, Phys. Rev. B **50**, 6465 (1994).

[11] A. Slawska-Wanieska, M. Gutowski, H. K. Lachowicz, T. Kulik, and H. Matyja, Phys. Rev. B **45**, 15 594 (1992).